Chem. Chem. Technol., 2024,
Vol. 18, No. 2, pp. 119–130

Chemistry

ACTIVATED PERIODATES AND SODIUM PERCARBONATE IN ADVANCED OXIDATION PROCESSES OF ORGANIC POLLUTANTS IN AQUEOUS MEDIA: A REVIEW

***Yuriy Sukhatskiy*[1, ✉], *Zenovii Znak*[1], *Martyn Sozanskyi*[1], *Mariana Shepida*[1], *Parag R. Gogate*[2], *Volodymyr Tsymbaliuk*[1]**

https://doi.org/10.23939/chcht18.02.119

Abstract. The methods of periodates and sodium percarbonate activation are considered for planning strategic approaches to increasing the efficiency and intensity of oxidative degradation of organic pollutants in aquatic environments. A classification of periodate activation methods is proposed, including activation methods by external energy effects, catalytic activation methods, and other activation methods (*e. g.*, by hydrogen peroxide, by hydroxylamine, activation in alkaline medium). Activation methods for sodium percarbonate were divided into homogeneous and heterogeneous activation methods.

Keywords: activation; periodate; sodium percarbonate; advanced oxidation processes; ultrasound; catalyst.

1. Introduction

The periodate ion (IO_4^-) is an oxidant with a redox potential of +1.6 V[1]. The main disadvantage of direct periodate oxidation is its selectivity. Thus, periodates are primarily used for the oxidation of alcohols, aldehydes, ketones, and carboxylic acids, that is, organic compounds with vicinal groups. Therefore, these oxidants need to be activated to expand the spectrum of organic pollutants in aqueous media that can be effectively oxidized using periodates.

Sodium percarbonate, like periodates, has significant potential for use in water purification technologies. It serves as a carrier of "solid hydrogen peroxide". Unlike liquid hydrogen peroxide, sodium percarbonate is thermally more stable, exhibits oxidative properties over a wider range of pH values, and the costs of its storage and transportation are significantly lower. The oxidative efficiency of sodium percarbonate can be significantly enhanced through its activation, which is accompanied by the generation of additional reactive oxygen species.

The focus of this review is aimed at familiarization with the activation methods of periodates and sodium percarbonate, as well as the corresponding advanced oxidation processes of organic pollutants in aqueous media.

2. Activation of Periodates

Among the strategic approaches to activate periodates, the use of three main ones can be distinguished: i) external energy influences (ultraviolet or visible irradiation, thermal energy); ii) catalysts (based on metals or their compounds, based on carbon and its compounds); iii) other activation methods (by hydrogen peroxide, in an alkaline medium, by hydroxylamine).

2.1. Activation by External Energy Effect

2.1.1. Activation by Ultraviolet or Visible Irradiation

Compared to those advanced oxidation processes, during the realization of which only hydroxyl radicals are generated, a variety of reactive species are formed as a result of photoactivation of periodates by UV irradiation. For example, at pH=5, as a result of periodates activation by UV irradiation, intermediates such as iodyl ($IO_3^\bullet$), periodyl ($IO_4^\bullet$), hydroxyl radicals ($^\bullet OH$), and atomic oxygen ($O(^3P)$) are formed. The final products of periodate photolysis are iodate ions (IO_3^-), oxygen (O_2), ozone (O_3), and hydrogen peroxide (H_2O_2). Among the mechanisms of periodate photoactivation, the most cited is the mechanism proposed by Wagner and Strehlow[3] (pH=5):

Initiation

$$IO_4^- + h\nu \rightarrow IO_3^\bullet + O^{\bullet-},\ k_1=2.3\times10^{-3}\ s^{-1}, \quad (1)$$

$$IO_4^- + h\nu \rightarrow IO_3^- + O(^3P),\ k_2=1.5\times10^{-4}\ s^{-1}. \quad (2)$$

Propagation

$$O^{\bullet-} + H^+ \leftrightarrow {}^\bullet OH,\ k_3=10^8\ dm^3/mol\times s^{-1}, \quad (3)$$

$$^\bullet OH + IO_4^- \rightarrow OH^- + IO_4^\bullet,\ k_4=4.5\times10^8\ dm^3/mol\times s^{-1}, \quad (4)$$

[1] Lviv Polytechnic National University 12, S. Bandery str., Lviv 79013, Ukraine
[2] Institute of Chemical Technology, Matunga, Mumbai 40019, India
✉ *yurii.v.sukhatskyi@lpnu.ua*
© Sukhatskiy Y., Znak Z., Sozanskyi M., Shepida M., Gogate P. R., Tsymbaliuk V., 2024

$$IO_4^- + IO_3^\bullet \rightarrow IO_4^\bullet + IO_3^-,\ k_5=5.0\times10^8\ dm^3/mol\times s^{-1},\quad (5)$$

$$IO_3^- + {}^\bullet OH \rightarrow IO_3^\bullet + OH^-,\ k_6=2.9\times10^8\ dm^3/mol\times s^{-1},\quad (6)$$

$$O(^3P) + O_2 \rightarrow O_3,\ k_7=4.0\times10^9\ dm^3/mol\times s^{-1},\quad (7)$$

$$O_3 + IO_3^\bullet \rightarrow IO_4^\bullet + O_2,\ k_8=10^8\ dm^3/mol\times s^{-1}.\quad (8)$$

Termination

$$2{}^\bullet OH \rightarrow H_2O_2,\ k_9=5.0\times10^9\ dm^3/mol\times s^{-1},\quad (9)$$

$$2IO_3^\bullet \rightarrow I_2O_6,\ k_{10}=5.0\times10^8\ dm^3/mol\times s^{-1},\quad (10)$$

$$2IO_4^\bullet \rightarrow I_2O_8,\ k_{11}=4.7\times10^8\ dm^3/mol\times s^{-1},\quad (11)$$

$$2O(^3P) \rightarrow O_2,\ k_{12}=5.4\times10^{-34}\ cc^2\times molecule^{-2}\times s^{-1},\quad (12)$$

$$I_2O_6 + H_2O \rightarrow IO_4^- + IO_3^- + 2H^+,\ k_{13}=4.5\times10^8\ dm^3/mol\times s^{-1},\quad (13)$$

$$I_2O_8 + H_2O \rightarrow IO_4^- + IO_3^- + 2H^+ + O_2,\ k_{14}=1.5\times10^8\ dm^3/mol\times s^{-1}.\quad (14)$$

Under alkaline conditions[1] (pH=11), periodates exist in a hydrated dimeric form ($H_2I_2O_{10}^{4-}$). The result of its activation by UV irradiation is the formation of hydroxyl and iodyl radicals (Scheme 15).

$$H_2I_2O_{10}^{4-} + h\nu \rightarrow {}^\bullet OH + IO_3^\bullet.\quad (15)$$

These radicals play a key role in the oxidative degradation of organic pollutants in aqueous media.

The use of UV irradiation to activate sodium periodate (the initial $NaIO_4$ concentration in the reaction medium – 3×10^{-3} mol/dm^3) for 90 min made it possible to reach a degradation degree of the acid orange 10 azo dye, which was equal to 99.2 %[5]. The conditions of oxidative degradation were as follows: the initial dye concentration in its aqueous solution 50 mg/dm^3; temperature of the reaction medium 20±1 °C; initial pH 5.4; UV irradiation intensity 15 mW/cm^2. With a further increase in the initial concentration of sodium periodate in the reaction medium above 3×10^{-3} mol/dm^3, the rate of termination reactions increases (reactions (9)–(14)), leading to a slight decrease in the initial degradation rate of acid orange 10 dye (Fig. 1).

In photocatalytic systems (using photosensitive materials, such as TiO_2), periodates serve as quenchers of conduction band electrons to inhibit the rapid recombination of electrons and holes generated under UV irradiation[6]. Zhang *et al.*[7] used scavenging experiments to identify the contribution of reactive species (generated in the UV/TiO_2/periodate process) to the degradation of Rhodamine B dye and proposed the following sequence: $O_2^{\bullet-} > h^+ > IO_3^\bullet$ and $IO_4^\bullet > O(^3P) > {}^\bullet OH$.

It was established that when using UV/TiO_2/periodate process (the photo-reactor scheme is shown in Fig. 2) within 10 min, a complete (100 %) degradation of Orange G azo dye (initial dye concentration – 50 mg/dm^3; reaction volume – 400 mL) was achieved. The conditions of the experimental studies were as follows: pH~6.5; temperature 20±2 °C; periodate concentration 10^3 mg/dm^3; TiO_2 concentration 4×10^2 mg/dm^3; UV irradiation intensity 4750 μW/cm^2; wavelength of UV irradiation 254 nm. In this case, the degradation rate constant of the Orange G dye was 0.282 min^{-1}, and the electrical energy consumption was estimated at 2.21 kWhm^{-3}/Order.[8]

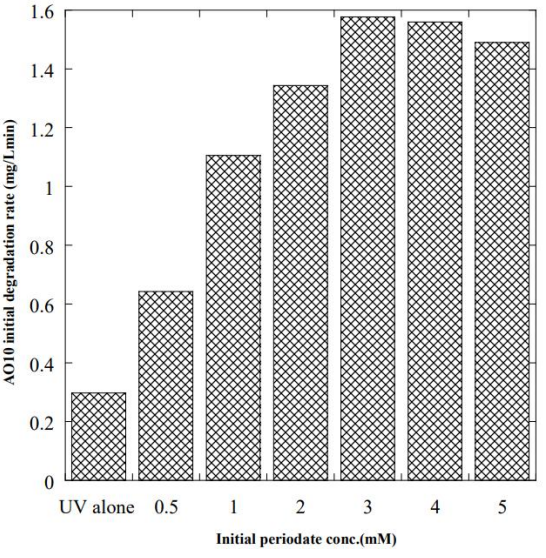

Fig. 1. Effect of the initial periodate concentration on the initial degradation rate of acid orange 10 ([acid orange 10]$_0$ = 50 mg/L, 20±1 °C, initial pH 5.4, UV irradiation intensity – 15 mW/cm^2)[5] under the terms of the Creative Commons CC BY license

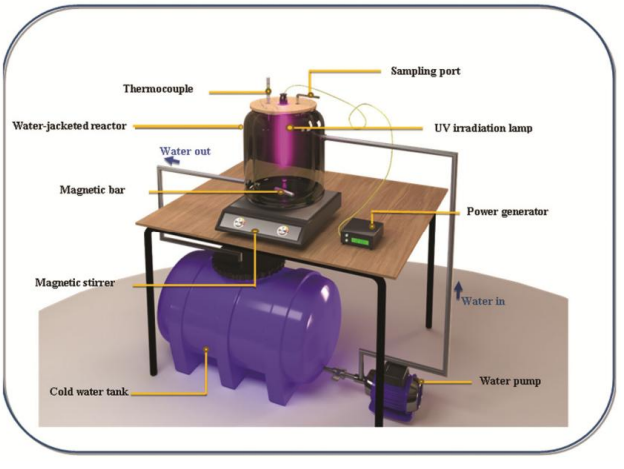

Fig. 2. The photo-reactor scheme for experimental studies of the degradation of Orange G azo dye using the UV/TiO_2/periodate process[8] under the terms of the Creative Commons CC BY license

Bendjama *et al.*[9] found a weak inhibitory effect of dissolved gases (O_2, Ar, N_2) on the degradation of Safranin O azine dye in water using the UV/TiO_2/periodate process.

New heterostructured photocatalysts ($AgIO_4/ZnO$, $AgIO_4/TiO_2$)[10, 11] with different $AgIO_4$ contents (from 5 to 20 wt. %) were synthesized for the degradation of dyes under visible light. For example, the $AgIO_4/TiO_2$ photocatalyst shows excellent photoactivity and stability during the degradation of Rhodamine B: using 0.3 g/dm^3 of photocatalyst with 10 wt. % of $AgIO_4$, a 98 % degradation degree of dye was achieved[11].

2.1.2. Thermal Activation

Lu *et al.*[12] proposed the thermo-activated periodate oxidation process (heat energy/periodate) for tetracycline degradation. It was found that the removal of tetracycline from water strongly depended on the temperature of the reaction medium. Thus, when using the heat energy/periodate process for 60 min with an initial pollutant concentration (tetracycline) in water of 50×10^{-6} mol/dm^3 and periodate of 500×10^{-6} mol/dm^3, and in the case of increasing the temperature of the reaction medium from 30 to 80 °C, the degree of tetracycline degradation increased from 18.1 to 89.3 %, and the rate constant of oxidative degradation increased from 0.003 to 0.036 min^{-1}. The activation energy of tetracycline degradation using the thermo-activated periodate oxidation process was 46.2 kJ/mol. Based on scavenging experiments and EPR experiments, it was confirmed that the main reactive oxygen species in the heat energy/periodate system were $IO_3^{\bullet}$, singlet oxygen ($^1O_2$), and $^{\bullet}OH$ (Fig. 3).

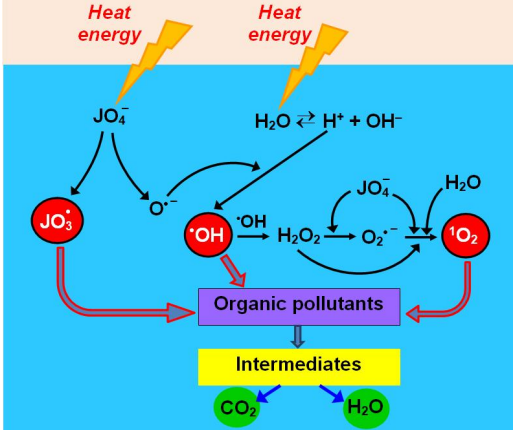

Fig. 3. The proposed mechanism of the thermo-activated periodate oxidation process (heat energy/periodate)

2.2. Activation by Catalysts

2.2.1. Activation by Transition Metals and Their Compounds

Transition metals and their compounds (most commonly oxides or sulfides) have excellent electron transfer capability and redox performance[6]. So, they can easily activate periodates to generate reactive oxygen species, which participate in the degradation of organic pollutants in aqueous media.

Various forms of iron (Fe^{2+}, nano zero-valent iron (nZVI))[13–15] and its compounds (α-Fe_2O_3[16], FeS[17]) are used for the efficient activation of periodates in oxidative degradation processes of phenol, its chloro- and nitro-derivatives, bisphenol A, and various pharmaceuticals (such as antibacterial and anti-inflammatory agents).

Iron (II) is oxidized to iron (III) by the periodate ion (Scheme 16) or by oxygen dissolved in the aqueous medium (Eq. 17) [18]:

$$Fe(II) + IO_4^- + H_2O \rightarrow Fe(III) + IO_3^- + O_2^{\bullet-} + 2H^+, \quad (16)$$

$$Fe(II) + O_2 \rightarrow Fe(III) + O_2^{\bullet-}. \quad (17)$$

In addition, the formation of Fe(IV) is possible (Eq. (18))[19]

$$Fe(II) + IO_4^- \rightarrow Fe(IV)O^{2+} + IO_3^-. \quad (18)$$

The values of standard redox potentials (E^0) for systems containing Fe(IV) were as follows[19]: $E^0(FeO^{2+}/FeO^+)$=1.30 eV; $E^0(FeO^{2+}/FeOH^{2+})$=1.95 eV; $E^0(FeO^{2+}/[Fe(H_2O)_6]^{3+})$=2.00 eV. Forms of Fe(IV), unlike hydroxyl radicals, are characterized by a long "lifetime": the half-life period is approximately ~7 s. Self-decomposition of Fe(IV) leads to the formation of Fenton-like systems (scheme 19)[20]

$$2Fe(IV) \rightarrow 1/3H_2O_2 + 2Fe(III) + 1/3O_2. \quad (19)$$

Excess of Fe(II) can lead to the "absorption effect" of Fe(IV) (Eq. 20)

$$Fe(IV) + Fe(II) \rightarrow 2Fe(III). \quad (20)$$

Therefore, as a result of the periodates activation by iron(II) compounds, a complex of oxidants is formed. The latter contains periodyl and iodyl radicals (results of hydroxyl radicals "capture" by periodate and iodate ions according to Eq. (4) and Eq. (6), respectively), superoxide radical anion, hydroxyl radicals, singlet oxygen, and compounds of Fe(III) and Fe(IV) with well-defined oxidative properties. This confirms the possibility of neutralizing the selectivity of periodate oxidation and, consequently, significantly increasing its efficiency and expanding the range of organic pollutants that are subject to degradation.

As a result of the periodate co-activation by the catalyst (α-Fe_2O_3) and visible irradiation (the vis-α-Fe_2O_3/periodate system), almost 100 % degradation of 4-chlorophenol was achieved within 60 min[16]. The degradation rate constant was 0.1015 min^{-1}. The experimental conditions were as follows: the initial concentration of 4-chlorophenol – 10^{-4} mol/dm^3; the initial concentration of periodate – 10^{-3} mol/dm^3; the α-Fe_2O_3 content in the reaction medium – 0.4 g/dm^3.

Besides iron-based catalysts, compounds of other transition metals are used to activate periodates: various

Mn species (Mn(II), Mn(III), and Mn(IV))[19,21,22], In_2O_3[23], Ru-supported Co_3O_4[24], sulfide-modified cobalt silicate[25].

2.2.2. Activation by Carbon-Based Materials

The carbon-based materials used to activate periodates include N-doped iron-based porous carbon (Fe@N-C)[26], pyrolyzed iron-nitrogen-carbon catalyst (FeNC)[27,28], visible-light-induced polymeric carbon nitride[29], atomically dispersed Co active sites supported by N-doped graphene[30], atomically dispersed Mn on carbon nanotubes[31], and sewage sludge-derived biochar[32–38].

Luo *et al.*[26] noted that the use of the Fe@N-C/periodate system for the degradation of sulfisoxazole (concentration in the reaction medium is 5 mg/dm^3) for 10 min resulted in a degree of pollutant degradation of 86.3 %. In this case, the degradation rate constant of sulfisoxazole was 0.196 min^{-1}. The conditions of the study were as follows: pH of the reaction medium 3.0; temperature 25 °C; initial concentration of periodate 0.5×10^{-3} mol/dm^3; catalyst content (Fe@N-C) in the reaction medium 0.05 g/dm^3. Based on the results of scavenging experiments, it was concluded that the reaction mechanism for the Fe@N-C/PI system involved electron transfer.

The use of the FeNC/periodate system for the degradation of organic micropollutants demonstrated high oxidation rates for phenol, 2,4,6-trichlorophenol, and Rhodamine B[27]. In this case, 100 % removal efficiency of these pollutants was achieved within 10 min.

For periodate activation, biochar obtained from pyrolysis of anaerobic sewage sludge at 800 °C (SBC-800) without any pretreatment was used. The use of the SBC-800/periodate system for the degradation of the azo dye Acid Orange 7 (initial concentration in the reaction medium – 20 mg/dm^3) over 90 min made it possible to reach a degradation degree of 97.6 %. The degradation rate constant of Acid Orange 7 was 0.0716 min^{-1}. The experimental conditions were as follows: pH of the reaction medium 3.0; temperature 25 °C; initial concentration of periodate 10^{-3} mol/dm^3; catalyst content (SBC-800) in the reaction medium 0.4 g/dm^3. It was found that singlet oxygen production and electron transfer mediated by the SBC-800-periodate complex were the dominant mechanisms for Acid Orange 7 oxidation[33].

2.3. Other Activation Methods

Other methods of periodate activation include activation by hydrogen peroxide, hydroxylamine, and activation in an alkaline medium.

The mechanism of periodate activation by hydrogen peroxide was considered in detail in our previous works[2,39]. The Peroxate process (H_2O_2/IO_4^-) was used for the oxidative degradation of thiazine dyes – Methylene blue[39] and Toluidine blue[40]. Chadi *et al.*[40] found that hydroxyl, iodyl radicals, and singlet oxygen play a key role in Toluidine blue degradation. Ultrasound intensifies heat and mass transfer processes, thereby enhancing the efficiency of organic pollutant degradation[39,41–45]. For example, the use of the ultrasound/H_2O_2/KIO_4 process (the Sonoperoxate process) for the oxidative degradation of Methylene blue for 60 min increased the degree of dye degradation by 18.5 % (from 55.6 to 74.1 %), compared to the use of the H_2O_2/KIO_4 process[39]. The research conditions were as follows: reaction volume 1 dm^3; pH ~7.0; initial temperature 17 °C; the initial concentration of Methylene blue 62.6×10^{-6} mol/dm^3; the molar ratio of Methylene blue: H_2O_2:KIO_4 = 1:100:25; ultrasonic power 180 W.

Using scavenging experiments and the spin-trapping electron paramagnetic resonance (EPR) technique, it was confirmed that the main reactive oxygen species of the periodate/hydroxylamine system were $^{\bullet}OH$, $HO_2^{\bullet}$ and $^1O_2$[46] The periodate/hydroxylamine system was used for the rapid (within 2 min) degradation of 4-chlorophenol and 2,4,6-trichlorophenol, as well as for the inactivation of Gram-positive (*S. aureus*) and Gram-negative (*E. coli*) bacteria with producing singlet oxygen as the dominant disinfectant.

In potassium periodate-based advanced oxidation processes, singlet oxygen was generated in alkaline conditions (pH greater than 8) by $O_2^{\bullet-}$ reacting with H_2O and IO_4^-[47]:

$$2O_2^{\bullet-} + 2H_2O \rightarrow {}^1O_2 + H_2O_2 + 2OH^-, \quad (21)$$

$$IO_4^- + 2O_2^{\bullet-} + H_2O \rightarrow IO_3^- + 2\,{}^1O_2 + 2OH^-. \quad (22)$$

3. Sodium Percarbonate Activation

Sodium percarbonate (SPC or peroxymonocarbonate of molecular form $Na_2CO_3\cdot1.5H_2O_2$) is characterized by a high redox potential value (1.8 V)[48]. Therefore, SPC is proposed to be used as an alternative to H_2O_2[49,50] solution for the oxidation of organic pollutants in natural and wastewater. Compared to liquid H_2O_2, which is used directly as an oxidant and based on which numerical variants of the Fenton process are implemented, SPC has many advantages: it can be used in a wide range of pH[51,52] (H_2O_2 as an oxidant has high oxidizing properties in a narrow range of pH = 2.5–3.0); it acts as a buffer[53]; characterized by high stability and explosion safety[4]; transportation and storage costs are much lower[54]. As a result of the SPC decomposition, non-toxic substances characteristic of natural aquatic environments (CO_2, water, sodium carbonate, and hydrogen carbonate) are formed. Therefore, its use allows to implement "green" technologies.

As a "solid" form of hydrogen peroxide, SPC can directly oxidize various pollutants in water, similar to H_2O_2. Oxidation of organic pollutants occurs due to the formation of hydroxyl radicals:

$$H_2O_2 \leftrightarrow 2^{\bullet}OH. \quad (23)$$

At the same time, part of the hydrogen peroxide decomposes with the formation of molecular oxygen, which has much less pronounced oxidizing properties:

$$2H_2O_2 \rightarrow 2H_2O + O_2. \quad (24)$$

The oxidation potential of hydroxyl radicals depends on pH and decreases from 2.8 at pH 3.0 to 1.5 V in an alkaline medium. However, carbonate ions included in SPC contribute to the transformation of hydroxyl radicals into other reactive radicals[55]. Thus, the oxidation potential of H_2O_2 increases in the system due to the formation of reactive peroxymonocarbonate[56]. As a result of the homolysis of the O–O bond, hydroxyl ($^{\bullet}OH$) and hydroperoxyl ($HO_2^{\bullet}$) radicals, anion radicals (carbonate – $CO_3^{\bullet-}$, and superoxide – $O_2^{\bullet-}$), singlet oxygen ($^1O_2$) are formed according to the following reactions:

$$HCO_3^- + H_2O_2 \rightarrow HCO_4^- + H_2O, \quad (25)$$

$$HCO_4^- \rightarrow CO_3^{\bullet-} + {}^{\bullet}OH, \quad (26)$$

$$CO_3^{\bullet-} + H_2O_2 \rightarrow HCO_3^- + HO_2^{\bullet}, \quad (27)$$

$$HO_2^{\bullet} \rightarrow O_2^{\bullet-} + H^+, \quad (28)$$

$$O_2^{\bullet-} + H_2O_2 \rightarrow {}^1O_2 + {}^{\bullet}OH + OH^-, \quad (29)$$

$$O_2^{\bullet-} + {}^{\bullet}OH \rightarrow {}^1O_2 + OH^-. \quad (30)$$

The effectiveness of the oxidizing action of SPC is significantly increased due to the action of catalysts and/or energy activation, which cause additional formation of hydroxyl, superoxide, carbonate ($E_{CO_3^{\bullet-}/CO_3^{2-}}$ = 1,78 V at pH 7.0) and other radicals[57]. According to the mechanism, SPC activation methods are divided into homogeneous and heterogeneous.

3.1. Homogeneous Activation of SPC

Methods of homogeneous SPC activation can be divided into physical and homogeneous catalytic methods.

3.1.1. Hydrodynamic Cavitation Activation of SPC

Hydrodynamic cavitation (HC) is one of the effective methods of neutralizing organic pollutants[58,59]. However, some pollutants, for example, estrogens, are resistant to the action of HC[60]. At the same time, the efficiency of advanced oxidation processes (AOPs) is significantly increased when using HC as an activating physical effect[61–63]. During an emergency, cavitation microbubbles appear, which subsequently collapse, leading to a local increase in temperature (10,000 K) and pressure (up to 1,000 MPa) [64]. As a result, water decomposes with the formation of reactive oxygen species (O, $^{\bullet}OH$, $HO_2^{\bullet}$)[65–67]. In addition, extremely high shear stresses and shock waves generated by the cavitation phenomenon occur during emergencies. They contribute to the destruction (sonolysis) of water with the formation of $^{\bullet}OH$ and $H^{\bullet}$ radicals and pollutants, primarily with a large molecular weight, with the formation of intermediate products. Intermediate compounds are more prone to interaction with radicals, for example, $^{\bullet}OH$, which increases the overall rate of degradation and/or mineralization of pollutants. $^{\bullet}OH$ radicals diffuse in the liquid and react with pollutant molecules, which leads to their oxidation/mineralization[64]. The synergistic effect of HC in combination with H_2O_2 was confirmed during the treatment of large volumes of wastewater at sewage treatment plants[62].

HC was used for the homogeneous activation of SPC in the processes of estrogen oxidation[60] due to the disintegration of SPC under conditions of high shear stress and multiphase bubble flow. In this work, it was also established that the decrease in estrogen concentration is observed for a long time after the cessation of the HC action, which lasted no more than 20 seconds. A similar effect was observed during the oxidative destruction of benzene (the degree of decomposition reached 98 %) in oxidizing conditions, which was explained by the radical mechanism of the process initiated with the help of HC[68].

The effectiveness of cavitation processes of pollutant destruction depends significantly on the structural features of the hydrodynamic cavitator[43–45,69]. Under optimal conditions of the process in the jet type HC, the efficiency of energy use reaches 93 %.

3.1.2. SPC Activation Using Ultrasound

The use of ultrasound in water purification is accompanied by the phenomenon of acoustic cavitation, which, like HC, generates hydroxyl radicals[70]. Therefore, the effect of ultrasound, which is mostly used together with other methods of SPC activation[71,72], is similar to that of HC. In particular, the simultaneous activation of SPC by ultrasound and ultraviolet irradiation (AOP – US/UV-LEDs/SPC) provided a synergistic effect during the oxidative degradation of the Acid Orange 7 dye due to an increase in the intensity of the formation of $^{\bullet}OH$ radicals[72] due to the participation of peroxymonocarbonate ions in this process (HCO_4^-). Due to the simultaneous action of ultrasound and ultraviolet in the reaction medium, both parallel and sequential processes are possible, which result in an increased yield of hydroxyl radicals[71]:

$$H_2O \rightarrow))) H^{\bullet} + {}^{\bullet}OH, \quad (31)$$

$$H^{\bullet} + H_2O_2 \rightarrow {}^{\bullet}OH + H_2O, \quad (32)$$

$$HCO_3^- + H_2O_2 \rightarrow HCO_4^- + H_2O, \quad (33)$$

$$HCO_4^- \rightarrow))){}^{\bullet}OH + CO_3^{\bullet -}, \quad (34)$$

$$HCO_4^- + h\nu \rightarrow {}^{\bullet}OH + CO_3^{\bullet -}, \quad (35)$$

$$HCO_4^- + H^{\bullet} \rightarrow {}^{\bullet}OH + HCO_3^-. \quad (36)$$

This ensured the degree of degradation of Acid Orange 7 dye 93.7 % at the power of ultrasound (20 kHz) 100 W, intensity of UV irradiation 2.55–2.71 mW/cm^3, pH 6.0, and activation time 5400 s[72].

Implementation of the modified sono-Fenton process (AOP – US/Fe^{2+}/SPC)[71] allowed to achieve a degree of the antibiotic metronidazole degradation of 90.2 % at an ultrasonic irradiation power of 140 W, time of 7 min, and the $FeSO_4$ concentration of 1 g/dm^3.

3.1.3. Activation of SPC by Contact Plasma

SPC activation occurs due to the interaction of electrons generated during the plasma discharge between the electrode above the surface of the solution and the surface of this solution with hydrogen peroxide to form $^{\bullet}OH$ radicals:

$$e^- + H_2O_2 \rightarrow OH^- + {}^{\bullet}OH. \quad (37)$$

The plasma generates UV irradiation, and ozone is formed in the air. These factors cause the formation of hydroxyl radicals according to the following main processes[73–75]:

$$H_2O_2 + h\nu \rightarrow 2{}^{\bullet}OH, \quad (38)$$

$$H_2O_2 + O_3 \rightarrow HO_2^- + O_2 + {}^{\bullet}OH, \quad (39)$$

$$O_3 + OH^- \rightarrow HO_2^- + 2{}^{\bullet}O, \quad (40)$$

$$^{\bullet}O + H_2O \rightarrow 2{}^{\bullet}OH. \quad (41)$$

SPC with a concentration of 0.12×10^{-3} mol/dm^3, activated by plasma (AOP – P/SPC) at a voltage of 18 kV for 1800 s made it possible to reduce the content of dimethyl phthalate in an aqueous solution by 92.1 % (initial concentration was 1 g/dm^3. The authors believe that the oxidative degradation of dimethyl phthalate occurred due to hydroxyl radicals, superoxide anion radicals, singlet oxygen, and carbonate anion radicals[73], which can be formed during the interaction of a carbonate ion with a hydroxyl radical, the generation of which was considered above:

$$CO_3^{2-} + {}^{\bullet}OH \rightarrow OH^- + CO_3^{\bullet -}. \quad (42)$$

As a result of SPC activation by a plasma discharge, the degree of tetracycline degradation was reached 94.3 % (voltage 4.8 kV; time 300 s; tetracycline initial concentration 20 mg/dm^3, SPC initial concentration 52×10^{-6} mol/dm^3)[74].

The complex mechanism of SPC activation by a plasma discharge and its interaction with pollutants can be depicted schematically (Fig. 4).

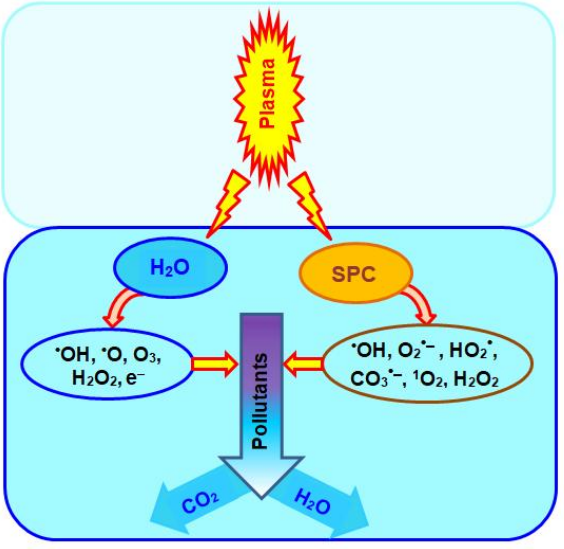

Fig. 4. Proposed mechanism for the plasma-involved SPC oxidation of contaminants

3.1.4. Activation of SPC by Ultraviolet Irradiation

Under the action of ultraviolet (UV) irradiation in an aqueous medium of hydrogen peroxide as a component of SPC decomposes with the formation of hydroxyl radicals[76]:

$$H_2O_2 + h\nu \leftrightarrow 2{}^{\bullet}OH. \quad (43)$$

They further react with carbonate/hydrogen carbonate ions with the formation of carbonate radicals according to Eqs. (44)–(45):

$$^{\bullet}OH + CO_3^{2-} \rightarrow CO_3^{\bullet -} + OH^-, \quad (44)$$

$$^{\bullet}OH + HCO_3^- \rightarrow CO_3^{\bullet -} + H_2O. \quad (45)$$

Due to the high redox potential, carbonate radicals can oxidize organic pollutants in water. For example, under the action of UV irradiation (AOP – UV/SPC), the degree of bisphenol A degradation reached 87.8 %[76]. The use of this AOP ensured the degradation of other compounds containing aromatic groups such as naphthalene[77], albendazole[78], aniline[79], and ciprofloxacin hydrochloride[80].

In the modified photo-Fenton process using SPC (AOP – UV/Fe^{2+}/SPC), effective oxidative degradation of both polycyclic aromatic compounds[81,82] and dyes, in particular, Acid Green 16[83], occurred. Hydroxyl radicals in this process are additionally generated with the participation of iron (II) ions[81]

$$Fe^{2+} + H_2O_2 + h\nu \rightarrow Fe^{3+} + {}^{\bullet}OH + OH^-. \quad (46)$$

However, advanced photochemical processes using SPC are appropriate for the treatment of water environments without suspended particles.

3.1.5. Activation of SPC by Metal Ions

To activate SPC, compounds containing metal ions with variable oxidation states (Me^{n+}), which interact with hydrogen peroxide, are used. This generates not only hydroxyl radicals but also a superoxide anion radical[49]:

$$Me^{n+} + H_2O_2 \rightarrow Me^{(n+1)+} + {}^{\bullet}OH + OH^-, \quad (47)$$

$$Me^{(n+1)+} + HO_2^- \rightarrow Me^{n+} + O_2^{\bullet-} + H^+. \quad (48)$$

The rate of reaction (47) increases with the increase in the concentration of metal ions in the reaction medium and decreases in the series $Co^{2+} > Mn^{2+} > Fe^{2+} > Fe^{3+} > Cu^{2+}$.[49]. The introduction of spirits or other aprotic solvents into aqueous systems increases the reactivity and, as a result, the degree of tetrachloromethane degradation[84]. The efficiency of organic compounds (AOP – Fe^{2+}/SPC) oxidation increases due to the addition of compounds capable of forming chelates to aqueous media: oxalic or citric acids, glutamate, and cysteine[85,86]. Enhancement of the oxidative action of Fe^{3+}/Fe^{2+} ions was also obtained by introducing tungsten dioxide into the reaction system as a co-catalyst for the decomposition of SPC and oxidation of metronidazole, which, under optimal conditions, was completely removed within 10 min[87].

These processes can be implemented in a narrow pH range, which is their significant drawback.

3.2. Heterogeneous Activation of SPC

Homogeneous processes, in which SPC is activated by metal ions, are limited by a narrow range of pH values and the lack of the possibility of reusing the catalyst, in particular, Fe^{2+}. This drawback was eliminated by using molybdenum powder[88]. In this system, sulfamethoxazole (SMX) degraded almost completely in 60 min, and the process rate was significantly higher than that without dispersed molybdenum. SMX oxidation involved hydroxyl (at pH 7.0 it played a dominant role), carbonate, and superoxide radicals, which were formed according to the following schemes:

$$Mo^0/Mo^{4+} + Fe^{3+} \rightarrow Fe^{2+} + Mo^{4+}/Mo^{6+}, \quad (49)$$

$$Fe^{2+} + H_2O_2 \rightarrow Fe^{3+} + 2{}^{\bullet}OH, \quad (50)$$

$${}^{\bullet}OH + CO_3^{2-} \rightarrow OH^- + CO_3^{\bullet-}, \quad (51)$$

$$CO_3^{\bullet-} + H_2O_2 \rightarrow HO_2^{\bullet} + HCO_3^-, \quad (52)$$

$$HO_2^{\bullet} \rightarrow H^+ + O_2^{\bullet-}, \quad (53)$$

$$Fe^{2+} + O_2 \rightarrow Fe^{3+} + O_2^{\bullet-}, \quad (54)$$

$$O_2^{\bullet-} + Mo^{6+}/{}^{\bullet}OH \rightarrow Mo^{4+} + {}^1O_2. \quad (55)$$

The high stability of Mo particles and the possibility of their reuse were revealed.

Zero-valent molybdenum was also used in the synthesis of Mo/carbon composites with a core-shell structure and in the form of nanorods for the activation of sodium percarbonate. The MoCN-600/SPC system was used for the efficient degradation of tetracycline[89]. Using the EPR method, it was established that the dominant type of active oxygen was the carbonate radical anion. Compared to H_2O_2, the MoCN-600/SPC system has significantly higher catalytic activity during the decomposition of tetracycline in a wider pH range.

Copper-modified zeolites also proved to be an effective SPC activator in tetracycline removal processes[90]. Active oxygen was in the form of ${}^{\bullet}OH$, ${}^1O_2$, $CO_3^{\bullet-}$ and $O_2^{\bullet-}$.

An advanced process involving a heterogeneous copper compound (CuO/SPC/AA, AA – ascorbic acid) was implemented for the oxidative degradation of sulfamethazine in a wide pH range (3.0–9.0)[91]. The main form of active oxygen in an acidic medium was the hydroxyl radical. In a neutral and alkaline media, it plays a secondary role, which is formed as a result of Cu(III) hydrolysis.

The use of zero-valent iron as the SPC activator in the Fenton-like processes of organic pollutants degradation is rather reduced to a donor of iron(II) ions[92,93]

$$2Fe^0 + O_2 + 2H^+ \rightarrow Fe^{2+} + H_2O_2 \quad (56)$$

with the simultaneous generation of additional amounts of the oxidant – hydrogen peroxide. Therefore, catalysis with the participation of zero-valent iron particles can be attributed to a mixed heterogeneous-homogeneous method of SPC activation. Bimetallic Fe^0/Co^0 particles deposited on TEMPO-oxidized cellulose nanofibers (TOCNF Fe/Cu) were used to activate SPC in the processes of chloroform oxidative degradation from groundwater[94]. In a neutral medium, the removal of chloroform exceeded 97.3 % within 180 min. The main role in oxidation was played by $O_2^{\bullet-}$ and ${}^{\bullet}OH$.

Natural zeolite[95] was used as a nanoscale zero-valent iron (nZVI) carrier used for SPC activation. With the help of the NZ-nZVI/SPC system, the majority (more than 90 %) of dyes are removed from water within 180 min. By increasing the loading of nZVI and the SPC concentration, a significant degree of bisphenol (BPA) degradation is achieved[96]. As a result of surface corrosion, iron(II) and (III) ions are released and radicals are generated, the first of which was dominant in the process of BPA oxidation.

The complex action of iron and copper as SPC activators is shown on the example of chalcopyrite $CuFeS_2$[97]. It is considered as a “green catalyst” – a donor of iron and copper sulfides. Due to the mixed valence of copper and iron, a very efficient transfer of electrons is achieved, which is important in oxidation processes. Therefore, with the participation of $CuFeS_2$, AOP is im-

plemented as a variant of Fenton's reaction. Surface ions Cu^{+} and Fe^{2+} of chalcopyrite play a major role in the activation of SPC[90]. In addition, this catalyst contributes to the generation of $O_2^{\bullet-}$, and $^{\bullet}OH$. The formed sulfide ion together with the interaction between Cu^{+} and Fe^{3+} contribute to Fe^{3+}/ Fe^{2+} cycles on the catalyst surface, which has a positive effect on the generation of reactive oxygen species.

4. Conclusions

This review focuses primarily on the activation methods of periodates and SPC. Methods of periodate activation were proposed to be classified into methods of activation by external energy effects (ultraviolet or visible irradiation, thermal energy), methods of catalytic activation (by transition metals or their compounds, by carbon-based materials), and other activation methods (by hydrogen peroxide, by hydroxylamine, in alkaline conditions). Methods of SPC activation were divided into homogeneous methods (using hydrodynamic cavitation, ultrasound; by contact plasma; by UV irradiation; by metal ions) and heterogeneous methods (by solid dispersed metal/bimetal particles, including immobilized on zeolite; by natural minerals, such as chalcopyrite) of activation. It was established that the qualitative composition of reactive oxygen species generated during the activation of periodates or SPC is determined by the activation method. Considering the need to follow the principles of energy- and resource-saving during the development of advanced oxidation processes for organic pollutants in aqueous media, the most reasonable are strategic approaches for oxidant activation, which are based on combinations of external energy effects with catalysts (transition metals or their compounds, carbon-based materials).

Acknowledgments

The authors acknowledge the funding of the Ministry of Education and Science of Ukraine for the scientific research project of young scientists "Advanced oxidation processes, including nanocatalytic, based on cavitation technologies for purification of aqueous media from resistant N-substituted organic compounds" (state registration number 0122U000790).

References

[1] Zhang, X.; Yu, X.; Yu, X.; Kamali, M.; Appels, L.; Van der Bruggen, B.; Cabooter, D.; Dewil, R. Efficiency and mechanism of 2,4-dichlorophenol degradation by the UV/ IO_4^- process. *Sci. Total Environ.* **2021**, *782*, 146781. https://doi.org/10.1016/j.scitotenv.2021.146781

[2] Sukhatskiy, Y.; Shepida, M.; Sozanskyi, M.; Znak, Z.; Gogate, P.R. Periodate-based advanced oxidation processes for wastewater treatment: A review. *Sep. Purif. Technol.* **2023**, *304*, 122305. https://doi.org/10.1016/j.seppur.2022.122305

[3] Djaballah, M.L.; Merouani, S.; Bendjama, H.; Hamdaoui, O. Development of a free radical-based kinetics model for the oxidative degradation of chlorazol black in aqueous solution using periodate photoactivated process. *J. Photochem. Photobiol. A: Chem.* **2021**, *408*, 113102. https://doi.org/10.1016/j.jphotochem.2020.113102

[4] Chen, L.; Duan, J.; Du, P.; Sun, W.; Lai, B.; Liu, W. Accurate identification of radicals by in-situ electron paramagnetic resonance in ultraviolet-based homogenous advanced oxidation processes. *Water Res.* **2022**, *221*, 118747. https://doi.org/10.1016/j.watres.2022.118747

[5] Nessaibia, M.; Ghodbane, H.; Ferkous, H.; Merouani, S.; Alam, M.; Balsamo, M.; Benguerba, Y.; Erto, A. Homogenous UV/periodate process for the treatment of acid orange 10 polluted water. *Water* **2023**, *15*, 758. https://doi.org/10.3390/w15040758

[6] Niu, L.; Zhang, K.; Jiang, L.; Zhang, M.; Feng, M. Emerging periodate-based oxidation technologies for water decontamination: A state-of-the-art mechanistic review and future perspectives. *J. Environ. Manag.* **2022**, *323*, 116241. https://doi.org/10.1016/j.jenvman.2022.116241

[7] Zhang, X.; Kamali, M.; Uleners, T.; Symus, J.; Zhang, S.; Liu, Z.; V. Costa, M.E.; Appels, L.; Cabooter, D.; Dewil, R. UV/TiO_2/periodate system for the degradation of organic pollutants – Kinetics, mechanisms and toxicity study. *Chem. Eng. J.* **2022**, *449*, 137680. https://doi.org/10.1016/j.cej.2022.137680

[8] Chamekh, H.; Chiha, M.; Ahmedchekkat, F.; Souames, N.E.H. Degradation of Orange G by UV/TiO_2/ IO_4^- process: Effect of operational parameters and estimation of electrical energy consumption. *Ind. J. Chem. Technol.* **2023**, *30*, 293–307. https://doi.org/10.56042/ijct.v30i3.62814

[9] Bendjama, M.; Hamdaoui, O.; Ferkous, H.; Alghyamah, A. Degradation of Safranin O in water by UV/TiO_2/ IO_4^- process: Effect of operating conditions and mineralization. *Catal.* **2022**, *12*, 1460. https://doi.org/10.3390/catal12111460

[10] Abdel-Aziz, R.; Ahmed, M.A.; Abdel Messih, M.F. A novel UV and visible light driven photocatalyst $AgIO_4$/ZnO nanoparticles with highly enhanced photocatalytic performance for removal of rhodamine B and indigo carmine dyes. *J. Photochem. Photobiol. A: Chem.* **2020**, *389*, 112245. https://doi.org/10.1016/j.jphotochem.2019.112245

[11] Ahmed, M.A.; Mahran, B.M.; Abbas, A.M.; Tarek, M.A.; Saed, A.M. Construction of direct Z-scheme $AgIO_4$/TiO_2 heterojunctions for exceptional photodegradation of rhodamine B dye. *J. Dispers. Sci. Technol.* **2020**, *43*, 349–363. https://doi.org/10.1080/01932691.2020.1841652

[12] Lu, G.; Li, X.; Li, W.; Liu, Y.; Wang, N.; Pan, Z.; Zhang, G.; Zhang, Y.; Lai B. Thermo-activated periodate oxidation process for tetracycline degradation: Kinetics and byproducts transformation pathways. *J. Hazard. Mater.* **2024**, *461*, 132696. https://doi.org/10.1016/j.jhazmat.2023.132696

[13] Zong, Y.; Shao, Y.; Zeng, Y.; Shao, B.; Xu, L.; Zhao, Z.; Liu, W.; Wu, D. Enhanced oxidation of organic contaminants by iron(II)-activated periodate: The significance of high-valent iron–oxo species. *Environ. Sci. Technol.* **2021**, *55*, 7634–7642. https://doi.org/10.1021/acs.est.1c00375

[14] Seid-Mohammadi, A.; Asgari, G.; Shokoohi, R.; Baziar, M.; Mirzaei, N.; Adabi, S.; Partoei, K. Degradation of phenol using US/periodate/nZVI system from aqueous solutions. *Glob. Nest. J.* **2019**, *21*, 360–367. https://doi.org/10.30955/gnj.002990
[15] Zong, Y.; Zhang, H.; Shao, Y.; Ji, W.; Zeng, Y.; Xu, L.; Wu, D. Surface-mediated periodate activation by nano zero-valent iron for the enhanced abatement of organic contaminants. *J. Hazard. Mater.* **2022**, *423*, 126991. https://doi.org/10.1016/j.jhazmat.2021.126991
[16] Wu, Y.; Tan, X.; Zhao, J.; Ma, J. α-Fe_2O_3 mediated periodate activation for selective degradation of phenolic compounds via electron transfer pathway under visible irradiation. *J. Hazard. Mater.* **2023**, *454*, 131506. https://doi.org/10.1016/j.jhazmat.2023.131506
[17] Wang, Q.; Zeng, H.; Liang, Y.; Cao, Ye.; Xiao, Y.; Ma, J. Degradation of bisphenol AF in water by periodate activation with FeS (mackinawite) and the role of sulfur species in the generation of sulfate radicals. *Chem. Eng. J.* **2021**, *407*, 126738. https://doi.org/10.1016/j.cej.2020.126738
[18] He, L.; Yang, S.; Yang, L.; Shen, S.; Li, Y.; Kong, D.; Chen, Z.; Yang, S.; Wang, J.; Wu, L. *et al*. Ball milling-assisted preparation of sludge biochar as a novel periodate activator for nonradical degradation of sulfamethoxazole: Insight into the mechanism of enhanced electron transfer. *Environ. Pollut*. **2023**, *316*, 120620. https://doi.org/10.1016/j.envpol.2022.120620
[19] Yang, B.; Ma, Q.; Hao, J.; Huang, J.; Wang, Q.; Wang, D.; Zhang, J. Periodate-based advanced oxidation processes: A review focusing on the overlooked role of high-valent iron and manganese species. *Chemosphere* **2023**, *337*, 139442. https://doi.org/10.1016/j.chemosphere.2023.139442
[20] Xiang, L.; Almatrafi, E.; Yang, H.; Ye, H.; Qin, F.; Yi, H.; Fu, Y.; Huo, X.; Xia, W.; Li, H. et al. Coupled carbon structure and iron species for multiple periodate-based oxidation reaction. *Chem. Eng. J.* **2023**, *455*, 140560. https://doi.org/10.1016/j.cej.2022.140560
[21] Zong, Y.; Shao, Y.; Ji, W.; Zeng, Y.; Xu, J.; Liu, W.; Xu, L.; Wu, D. Trace Mn(II)-catalyzed periodate oxidation of organic contaminants not relying on any transient reactive species: The substrate-dependent dual roles of in-situ formed colloidal MnO_2. *Chem. Eng. J.* **2023**, *451*, 139106. https://doi.org/10.1016/j.cej.2022.139106
[22] Yu, J.; Qiu, W.; Lin, X.; Wang, Y.; Lu, X.; Yu, Y.; Gu, H.; Heng, S.; Zhang, H.; Ma, J. Periodate activation with stable $MgMn_2O_4$ spinel for bisphenol A removal: Radical and non-radical pathways. *Chem. Eng. J.* **2023**, *459*, 141574. https://doi.org/10.1016/j.cej.2023.141574
[23] Yang, T.; An, L.; Zeng, G.; Mai, J.; Li, Y.; Lian, J.; Zhang, H.; Li, J.; Cheng, X.; Jia, J. et al. Enhanced hydroxyl radical generation for micropollutant degradation in the In_2O_3/Vis-LED process through the addition of periodate. *Water Res.* **2023**, *243*, 120401. https://doi.org/10.1016/j.watres.2023.120401
[24] Zhang, K.; Ye, C.; Lou, Y.; Yu, X.; Feng, M. Promoting selective water decontamination via boosting activation of periodate by nanostructured Ru-supported Co_3O_4 catalysts. *J. Hazard. Mater.* **2023**, *442*, 130058. https://doi.org/10.1016/j.jhazmat.2022.130058
[25] Chen, W.; Dai, X.; Liu, Z.; Du, B.; Zheng, X.; Ma, D.; Huang, X. Sulfide-modified cobalt silicate activated periodate for nitenpyram degradation: Enhanced radical and non-radical pathway. *Chem. Eng. J.* **2023**, *469*, 143922. https://doi.org/10.1016/j.cej.2023.143922
[26] Luo, K.; Shi, Y.; Huang, R.; Wei, X.; Wu, Z.; Zhou, P.; Zhang, H.; Wang, Y.; Xiong, Z.; Lai, B. Activation of periodate by N-doped iron-based porous carbon for degradation of sulfisoxazole: Significance of catalyst-mediated electron transfer mechanism. *J. Hazard. Mater.* **2023**, *457*, 131790. https://doi.org/10.1016/j.jhazmat.2023.131790
[27] Long, Y.; Huang, S.; Zhao, S.; Xiao, G.; Sun, J.; Peng, D. Pyrolyzed iron-nitrogen-carbon hybrids for efficient contaminant decomposition via periodate activation: Active site and degradation mechanism. *Sep. Purif. Technol*. **2023**, *317*, 123945. https://doi.org/10.1016/j.seppur.2023.123945
[28] Shen, S.; Jiang, W.; Zhao, Q.; He, L.; Ma, Y.; Zhou, X.; Wang, J.; Yang, L.; Chen, Z. Molten-salts assisted preparation of iron-nitrogen-carbon catalyst for efficient degradation of acetaminophen by periodate activation. *Sci. Total Environ*. **2023**, *859*, 160001. http://dx.doi.org/10.1016/j.scitotenv.2022.160001
[29] Chen, Y.; Yuan, X.; Jiang, L.; Zhao, Y.; Chen, H.; Shangguan, Z.; Qin, C.; Wang, H. Insights into periodate oxidation of antibiotics mediated by visible-light-induced polymeric carbon nitride: Performance and mechanism. *Chem. Eng. J.* **2023**, *457*, 141147. https://doi.org/10.1016/j.cej.2022.141147
[30] Long, Y.; Dai, J.; Zhao, S.; Su, Y.; Wang, Z.; Zhang, Z. Atomically dispersed cobalt sites on graphene as efficient periodate activators for selective organic pollutant degradation. *Environ. Sci. Technol.* **2021**, *55*, 5357–5370. https://doi.org/10.1021/acs.est.0c07794
[31] Hu, J.; Zou, Y.; Li, Y.; Yu, Z.; Bao, Y.; Lin, L.; Li, B.; Li, X.-Y. Periodate activation by atomically dispersed Mn on carbon nanotubes for the production of iodate radicals and rapid degradation of sulfadiazine. *Chem. Eng. J.* **2023**, *472*, 144862. https://doi.org/10.1016/j.cej.2023.144862
[32] He, L.; Lv, L.; Pillai, S.C.; Wang, H.; Xue, J.; Ma, Y.; Liu, Y.; Chen, Y.; Wu, L.; Zhang, Z. et al. Efficient degradation of diclofenac sodium by periodate activation using Fe/Cu bimetallic modified sewage sludge biochar/UV system. *Sci. Total Environ.* **2021**, *783*, 146974. https://doi.org/10.1016/j.scitotenv.2021.146974
[33] Xiao, P.; Yi, X.; Wu, M.; Wang, X.; Zhu, S.; Gao, B.; Liu, Y.; Zhou, H. Catalytic performance and periodate activation mechanism of anaerobic sewage sludge-derived biochar. *J. Hazard. Mater.* **2022**, *424*, 127692. https://doi.org/10.1016/j.jhazmat.2021.127692
[34] Yang, H.; Liu, Y.; Zhang, Y.; Liu, L.; Xia, S.; Xue, Q. Secondary pyrolysis oil-based drill-cutting ash for peroxymonosulfate/periodate activation to remove tetracycline: A comparative study. *Sep. Purif. Technol*. **2022**, *294*, 121264. https://doi.org/10.1016/j.seppur.2022.121264
[35] He, L.; Shi, Y.; Chen, Y.; Shen, S.; Xue, J.; Ma, Y.; Zheng, L.; Wu, L.; Zhang, Z.; Yang, L. Iron-manganese oxide loaded sludge biochar as a novel periodate activator for thiacloprid efficient degradation over a wide pH range. *Sep. Purif. Technol*. **2022**, *288*, 120703. https://doi.org/10.1016/j.seppur.2022.120703
[36] Fang, G.; Li, J.; Zhang, C.; Qin, F.; Luo, H.; Huang, C.; Qin, D.; Ouyang, Z. Periodate activated by manganese oxide/biochar composites for antibiotic degradation in aqueous system: Combined effects of active manganese species and biochar. *Environ. Pollut.* **2022**, *300*, 118939. https://doi.org/10.1016/j.envpol.2022.118939
[37] Dai, J.; Wang, Z.; Chen, K.; Ding, D.; Yang, S.; Cai, T. Applying a novel advanced oxidation process of biochar activated periodate for the efficient degradation of bisphenol A: Two nonradical pathways. *Chem. Eng. J.* **2023**, *453*, 139889. https://doi.org/10.1016/j.cej.2022.139889

[38] Hu, J.; Gong, H.; Liu, X.; Luo, J.; Zhu, N. Target-prepared sludge biochar-derived synergistic Mn and N/O induces high-performance periodate activation for reactive iodine radicals generation towards ofloxacin degradation. *J. Hazard. Mater.* **2023**, *460*, 132362. https://doi.org/10.1016/j.jhazmat.2023.132362
[39] Sukhatskiy, Y.; Sozanskyi, M.; Shepida, M.; Znak, Z.; Gogate, P.R. Decolorization of an aqueous solution of methylene blue using a combination of ultrasound and peroxate process. *Sep. Purif. Technol.* **2022**, *288*, 120651.
https://doi.org/10.1016/j.seppur.2022.120651
[40] Chadi, N.E.; Merouani, S.; Hamdaoui, O.; Bouhelassa, M.; Ashokkumar, M. H_2O_2/periodate (IO_4^-): a novel advanced oxidation technology for the degradation of refractory organic pollutants. *Environ. Sci.: Water Res. Technol.* **2019**, *5*, 1113–1123.
https://doi.org/10.1016/j.seppur.2022.120651
[41] Znak, Z.O.; Sukhatskiy, Y.V.; Zin, O.I.; Khomyak, S.V.; Mnykh, R.V.; Lysenko, A.V. The decomposition of the benzene in cavitation fields. *Voprosy Khimii i Khimicheskoi Tekhnologii* **2018**, *1*, 72–77.
[42] Znak, Z.O.; Sukhatskiy, Y.V.; Zin, O.I.; Vyrsta, K.R. The intensification of the cavitation decomposition of benzene. *Voprosy Khimii i Khimicheskoi Tekhnologii* **2019**, *4*, 55–61.
https://doi.org/10.32434/0321-4095-2019-125-4-55-61
[43] Yavorskiy, V.; Sukhatskiy, Y.; Znak, Z.; Mnykh, R. Investigations of cavitation processes in different types of emitters using sonochemical analysis. *Chem. Chem. Technol*. **2016**, *10*, 507–513.
https://doi.org/10.23939/chcht10.04.507
[44] Yavors'kyi, V.T.; Znak, Z.O.; Sukhats'kyi, Y.V.; Mnykh, R.V. Energy characteristics of treatment of corrosive aqueous media in hydrodynamic cavitators. *Mater. Sci.* **2017**, *52*, 595–600.
https://doi.org/10.1007/s11003-017-9995-8
[45] Znak, Z.; Sukhatskiy, Y. The brandon method in modelling the cavitation processing of aqueous media. *East.-Eur. J. Enterp. Technol.* **2016**, *3*, 37–42. https://doi.org/10.15587/1729-4061.2016.72539
[46] Sun, H.; He, F.; Choi, W. Production of reactive oxygen species by the reaction of periodate and hydroxylamine for rapid removal of organic pollutants and waterborne bacteria. *Environ. Sci. Technol.* **2020**, *54*, 6427–6437.
https://dx.doi.org/10.1021/acs.est.0c00817
[47] Xie, Z.-H.; He, C.-S.; Pei, D.-N.; Dong, Y.; Yang, S.-R.; Xiong, Z.; Zhou, P.; Pan, Z.-C.; Yao, G.; Lai, B. Review of characteristics, generation pathways and detection methods of singlet oxygen generated in advanced oxidation processes (AOPs). *Chem. Eng. J.* **2023**, *468*, 143778.
https://doi.org/10.1016/j.cej.2023.143778
[48] Yu, X.; Kamali, M.; Aken, P.V.; Appels, L.; Van der Bruggen, B.; Dewil, R. Synergistic effects of the combined use of ozone and sodium percarbonate for the oxidative degradation of dichlorvos. *J. Water Process Eng.* **2021**, *39*, 101721.
https://doi.org/10.1016/j.jwpe.2020.101721
[49] Ma, J.; Yang, X.; Jiang, X.; Wen, J.; Li, J.; Zhong, Y.; Chi, L.; Wang, Y. Percarbonate persistence under different water chemistry conditions. *Chem. Eng. J.* **2020**, *389*, 123422.
https://doi.org/10.1016/j.cej.2019.123422
[50] Hung, C.-M.; Chen, C.-W.; Huang, C.-P.; Tsai, M.-L.; Wu, C.-H.; Lin, Y.-L.; Cheng, Y.-R.; Dong, C.-D. Efficacy and cytotoxicity of engineered ferromanganese-bearing sludge-derived biochar for percarbonate-induced phthalate ester degradation. *J. Hazard. Mater.* **2022**, *422*, 126922. https://doi.org/10.1016/j.jhazmat.2021.126922
[51] Pimentel, J.A.I.; Dong, C.-D.; Garcia-Segura, S.; Abarca, R.R.M.; Chen, C.-W.; de Luna, M.D.G. Degradation of tetracycline antibiotics by Fe^{2+}-catalyzed percarbonate oxidation. *Sci. Total Environ*. **2021**, *781*, 146411.
https://doi.org/10.1016/j.scitotenv.2021.146411
[52] Huang, J.; Zhou, Z.; Ali, M.; Gu, X.; Danish, M.; Sui, Q.; Lyu, S. Degradation of trichloroethene by citric acid chelated Fe(II) catalyzing sodium percarbonate in the environment of sodium dodecyl sulfate aqueous solution. *Chemosphere* **2021**, *281*, 130798.
https://doi.org/10.1016/j.chemosphere.2021.130798
[53] Sablas, M.M.; de Luna, M.D.G.; Garcia-Segura, S.; Chen, C.-W.; Chen, C.-F.; Dong, C.-D. Percarbonate mediated advanced oxidation completely degrades recalcitrant pesticide imidacloprid: Role of reactive oxygen species and transformation products. *Sep. Purif. Technol.* **2020**, *250*, 117269.
https://doi.org/10.1016/j.seppur.2020.117269
[54] Ling, X.; Deng, J.; Ye, C.; Cai, A.; Ruan, S.; Chen, M.; Li, X. Fe(II)-activated sodium percarbonate for improving sludge dewaterability: Experimental and theoretical investigation combined with the evaluation of subsequent utilization. *Sci. Total Environ*. **2021**, *799*, 149382. https://doi.org/10.1016/j.scitotenv.2021.149382
[55] Li, Y.J.; Dong, H.R.; Xiao, J.Y.; Li, L.; Chu, D.D.; Hou, X.Z.; Xiang, S.X.; Dong, Q.X.; Zhang, H.X. Advanced oxidation processes for water purification using percarbonate: Insights into oxidation mechanisms, challenges, and enhancing strategies. *J. Hazard. Mater*. **2023**, *442*, 130014.
https://doi.org/10.1016/j.jhazmat.2022.130014
[56] Ma, J.; Xia, X.C.; Ma, Y.; Luo, Y.J.; Zhong, Y.J. Stability of dissolved percarbonate and its implications for groundwater remediation. *Chemosph*. **2018**, *205*, 41–44.
https://doi.org/10.1016/j.chemosphere.2018.04.084
[57] Zhang, B.T.; Kuang, L.L.; Teng, Y.G.; Fan, M.H.; Ma, Y. Application of percarbonate and peroxymonocarbonate in decontamination technologies. *J. Environ. Sci*. **2021**, *105*, 100–115.
https://doi.org/10.1016/j.jes.2020.12.031
[58] Thanekar, P.; Lakshmi, N.J.; Shah, M.; Gogate, P.R.; Znak, Z.; Sukhatskiy, Y.; Mnykh, R. Degradation of dimethoate using combined approaches based on hydrodynamic cavitation and advanced oxidation processes. *Process Saf. Environ. Prot*. **2020**, *143*, 222–230. https://doi.org/10.1016/j.psep.2020.07.002
[59] Thanekar, P.; Gogate, P.R. Improved processes involving hydrodynamic cavitation and oxidants for treatment of real industrial effluent. *Sep. Purif. Technol*. **2020**, *239*, 116563.
https://doi.org/10.1016/j.seppur.2020.116563
[60] Odehnalová, K.; Přibilová, P.; Maršálková, E.; Zezulka, Š.; Pochylý, F.; Rudolf, P.; Maršálek, B. Hydrodynamic cavitation-enhanced activation of sodium percarbonate for estrogen removal. *Water Sci. Technol*. **2023**, *88*, 2905–2916.
https://doi.org/10.2166/wst.2023.382
[61] Dular, M.; Griessler-Bulc, T.; Gutierrez-Aguirre, I.; Heath, E.; Kosjek, T.; Klemenčič, A.K.; Oder, M.; Petkovšek, M.; Rački, N.; Ravnikar M. et al. Use of hydrodynamic cavitation in (waste)water treatment. *Ultrason. Sonochem*. **2016**, *29*, 577–588.
https://doi.org/10.1016/j.ultsonch.2015.10.010
[62] Maršalek, B.; Zezulka, S.; Maršalkova, E.; Pochyly, F; Rudolf, P. Synergistic effects of trace concentrations of hydrogen peroxide used in a novel hydrodynamic cavitation device allows for selective removal of cyanobacteria. *Chem. Eng. J*. **2020**, *382*, 122383.
https://doi.org/10.1016/j.cej.2019.122383
[63] Panda, D.; Saharan, V.K.; Manickam, S. Controlled hydrodynamic cavitation: A review of recent advances and perspectives for greener processing. *Processes* **2020**, *8*, 220.
https://doi.org/10.3390/pr8020220
[64] Badve, M.; Gogate, P.; Pandit, A.; Csoka, L. Hydrodynamic cavitation as a novel approach for wastewater treatment in wood

finishing industry. *Sep. Purif. Technol*. **2013**, *106*, 15–21. https://doi.org/10.1016/j.seppur.2012.12.029
[65] Zheng, H.X.; Zheng, Y.; Zhu, J.S. Recent developments in hydrodynamic cavitation reactors: Cavitation mechanism, reactor design, and applications. *Eng*. **2022**, *19*, 180–198. https://doi.org/10.1016/j.eng.2022.04.027
[66] Amin, L.P.; Gogate, P.R.; Burgess, A.E.; Bremner, D.H. Optimization of a hydrodynamic cavitation reactor using salicylic acid dosimetry. *Chem. Eng. J*. **2010**, *156*, 165–169. https://doi.org/10.1016/j.cej.2009.09.043
[67] Kohno, M.; Mokudai, T.; Ozawa, T.; Niwano, Y. Free radical formation from sonolysis of water in the presence of different gases. *J. Clin. Biochem. Nutr*. **2011**, *49*, 96–101. https://doi.org/10.3164/jcbn.10-130
[68] Thanekar, P.; Gogate, P.R.; Znak, Z.; Sukhatskiy, Y.; Mnykh, R. Degradation of benzene present in wastewater using hydrodynamic cavitation in combination with air. *Ultrason. Sonochem*. **2021**, *70*, 105296. https://doi.org/10.1016/j.ultsonch.2020.105296
[69] Sukhatskiy, Y.; Znak, Z.; Zin, O.; Chupinskyi, D. Ultrasonic cavitation in wastewater treatment from azo dye methyl orange. *Chem. Chem. Technol*. **2021**, *15*, 284–290. https://doi.org/10.23939/chcht15.02.284
[70] Torres, R.A.; Pétrier, C.; Combet, E.; Carrier, M.; Pulgarin, C. Ultrasonic cavitation applied to the treatment of bisphenol A. Effect of sonochemical parameters and analysis of BPA by-products. *Ultrason. Sonochem*. **2008**, *15***,** 605–611. https://doi.org/10.1016/j.ultsonch.2007.07.003
[71] Lin, X.; He, J.; Xu, L.; Fang, Y.; Rao, G. Degradation of metronidazole by ultrasound-assisted sodium percarbonate activated by ferrous sulfate. *Water Pollut. Treat*. **2020**, *8*, 66–76. https://doi.org/10.12677/wpt.2020.83010
[72] Eslami, A.; Mehdipour, F.; Lin, K.-Y.A.; Maleksari, H.S.; Mirzaei, F.; Ghanbari, F. Sono-photo activation of percarbonate for the degradation of organic dye: The effect of water matrix and identification of by-products. *J. Water Process Eng*. **2020**, *33*, 100998. https://doi.org/10.1016/j.jwpe.2019.100998
[73] Wang, T.; Jia, H.; Guo, X.; Xia, T.; Qu, G.; Sun, Q.; Yin, X. Evaluation of the potential of dimethyl phthalate degradation in aqueous using sodium percarbonate activated by discharge plasma. *Chem. Eng. J*. **2018**, *346*, 65–76. https://doi.org/10.1016/j.cej.2018.04.024
[74] Tang, S.; Yuan, D.; Rao, Y.; Li, M.; Shi, G.; Gu, J.; Zhang, T. Percarbonate promoted antibiotic decomposition in dielectric barrier discharge plasma. *J. Hazard. Mater*. **2019**, *366*, 669–676. https://doi.org/10.1016/j.jhazmat.2018.12.056
[75] Geng, T.; Yi, C.; Yi, R.; Yang, L.; Nawaz, M.I. Mechanism and degradation pathways of bisphenol A in aqueous solution by strong ionization discharge. *Water Air Soil Pollut*. **2020**, *231*, 185. https://doi.org/10.1007/s11270-020-04563-5
[76] Gao, J.; Duan, X.; O'Shea, K.; Dionysiou, D.D. Degradation and transformation of bisphenol A in UV/sodium percarbonate: Dual role of carbonate radical anion. *Water Res*. **2020**, *171*, 115394. https://doi.org/10.1016/j.watres.2019.115394
[77] Qiu, Z.; Rao, G.; Wang, L.; Wang, L. Photo-assisted degradation of naphthalene by sodium percarbonate system. *Adv. Environ. Prot*. **2021**, *11*, 497–505. https://doi.org/10.12677/AEP.2021.113055
[78] Ortiz-Marin, A.D.; Bandala, E.R.; Ramírez, K.; Moeller-Chávez, G.; Pérez-Estrada, L.; Ramírez-Pereda, B.; Amabilis-Sosa, L.E. Kinetic modeling of UV/H_2O_2, UV/sodium percarbonate, and UV/potassium peroxymonosulfate processes for albendazole degradation. *Reac. Kinet. Mech. Catal*. **2022**, *135*, 639–654. https://doi.org/10.1007/s11144-021-02152-z
[79] Li, L.; Guo, R.; Zhang, S.; Yuan, Y. Sustainable and effective degradation of aniline by sodium percarbonate activated with UV in aqueous solution: Kinetics, mechanism and identification of reactive species. *Environ. Res*. **2022**, *207*, 112176. https://doi.org/10.1016/j.envres.2021.112176
[80] Mohammadi, S.; Moussavi, G.; Yaghmaeian, K.; Giannakis, S. Development of a percarbonate-enhanced Vacuum UV process for simultaneous fluoroquinolone antibiotics removal and fecal bacteria inactivation under a continuous flow mode of operation. *Chem. Eng. J*. **2022**, *431*, 134064. https://doi.org/10.1016/j.cej.2021.134064
[81] Kozak, J.; Włodarczyk-Makuła, M. The use of sodium percarbonate in the Fenton reaction for the PAHs oxidation. *Civ. Environ. Eng. Rep*. **2018**, *28*, 124–139. https://doi.org/10.2478/ceer-2018-0024
[82] Kozak, J.; Włodarczyk-Makuła, M. The use of sodium carbonate-hydrogen peroxide (2/3) in the modified Fenton reaction to degradation PAHs in coke wastewater. *Proc*. **2019**, *16*, 44–48. https://doi.org/10.3390/proceedings2019016044
[83] Pieczykolan, B.; Płonka, I.; Barbusiński, K. Discoloration of dye wastewater by modified UV-Fenton process with sodium percarbonate. *Archit. Civ. Eng. Environ*. **2016**, *9*, 135–140. https://doi.org/10.21307/acee-2016-060
[84] Tang, P.; Jiang, W.; Lu, S.; Zhang, X.; Xue, Y.; Qiu, Z.; Sui, Q. Enhanced degradation of carbon tetrachloride by sodium percarbonate activated with ferrous ion in the presence of ethyl alcohol. *Environ. Technol*. **2019**, *40*, 356–364. https://doi.org/10.1080/09593330.2017.1393012
[85] Farooq, U.; Sajid, M.; Shan, A.; Wang, X.; Lyu, S. Role of cysteine in enhanced degradation of trichloroethane under ferrous percarbonate system. *Chem. Eng. J*. **2021**, *423*, 130221. https://doi.org/10.1016/j.cej.2021.130221
[86] Fu, X.; Wei, X.; Zhang, W.; Yan, W.; Wei, P.; Lyu, S. Enhanced effects of reducing agent on oxalate chelated Fe(II) catalyzed percarbonate system for benzene degradation. *Water Supply* **2022**, *22*, 208–219. https://doi.org/10.2166/ws.2021.278
[87] Pan, S.; Zhao, T.; Liu, H.; Li, X.; Zhao, M.; Yuan, D.; Jiao, T.; Zhang, Q.; Tang, S. Enhancing ferric ion/sodium percarbonate Fenton-like reaction with tungsten disulfide cocatalyst for metronidazole decomposition over wide pH range. *Chem. Eng. J*. **2023**, *452*, 139245. https://doi.org/10.1016/j.cej.2022.139245
[88] Zhou, Z.; Ye, G.; Zong, Y.; Zhao, Z.; Wu. D. Improvement of Fe(III)/percarbonate system by molybdenum powder and tripolyphosphate: Co-catalytic performance, low oxidant consumption, pH-dependent mechanism. *J. Hazard. Mater*. **2024**, *464*, 132924. https://doi.org/10.1016/j.jhazmat.2023.132924
[89] Pang, K.; Fang, G.; Wang, Y.; Huang, Y.; Huang, D.; Liu, X. Synthesis of Mo-based/carbon nanocomposistes for water decontamination *via* percarbonate activation. *Catal. Lett*. **2024**, *154*, 2999–3008. https://doi.org/10.1007/s10562-023-04517-6
[90] Li, Y.; Dong, H.; Li, L.; Xiao, J.; Xiao, S.; Jin, Z. Efficient degradation of sulfamethazine via activation of percarbonate by chalcopyrite. *Water Res*. **2021**, *202*, 117451. https://doi.org/10.1016/j.watres.2021.117451
[91] Li, Y.; Dong, H.; Xiao, J.; Li, L.; Dong, J.; Huang, D.; Deng, J. Ascorbic acid-enhanced CuO/percarbonate oxidation: Insights into the pH-dependent mechanism. *ACS ES&T Eng*. **2023**, *3*, 798–810. https://doi.org/10.1021/acsestengg.2c00410

[92] Liu, M.; Ye, Y.; Xu, L.; Gao, T.; Zhong, A.; Song, Z. Recent advances in nanoscale zero-valent iron (nZVI)-based advanced oxidation processes (AOPs): Applications, mechanisms, and future prospects. *Nanomaterials* **2023**, *13*, 2830. https://doi.org/10.3390/nano13212830
[93] Makido, O.; Khovanets', G.; Kochubei, V.; Yevchuk, I. Nanostructured magnetically sensitive catalysts for the Fenton system: Obtaining, research, application. *Chem. Chem. Technol*. **2022**, *16*, 227–236. https://doi.org/10.23939/chcht16.02.227
[94] Che, M.; Xiao, J.; Shan, C.; Chen, S.; Huang, R.; Zhou, Y.; Cui, M.; Qi, W.; Su, R. Efficient removal of chloroform from groundwater using activated percarbonate by cellulose nanofiber-supported Fe/Cu nanocomposites. *Water Res*. **2023**, *243*, 120420. https://doi.org/10.1016/j.watres.2023.120420
[95] Rashid, T.; Iqbal, D.; Hazafa, A.; Hussain, S.; Sher, F.; Sher, F. Formulation of zeolite supported nano-metallic catalyst and applications in textile effluent treatment. *J. Environ. Chem. Eng*. **2020**, *8*, 104023. https://doi.org/10.1016/j.jece.2020.104023
[96] Xiao, Y.; Liu, X.; Huang, Y.; Kang, W.; Wang, Z.; Zheng, H. Roles of hydroxyl and carbonate radicals in bisphenol A degradation via a nanoscale zero-valent iron/percarbonate system: Influencing factors and mechanisms. *RSC Adv*. **2021**, *11*, 3636–3644. https://doi.org/10.1039/D0RA08395J
[97] Rostami-Javanroudi, S.; Fattahi, N.; Sharafi, K.; Arfaeinia, H.; Moradi, M. Chalcopyrite as an oxidants activator for organic pollutant remediation: A review of mechanisms, parameters, and future perspectives. *Heliyon* **2023**, *9*, e19992. https://doi.org/10.1016/j.heliyon.2023.e19992

Received: March 05, 2024 / Revised: April 26, 2024 / Accepted: May 02, 2024

АКТИВОВАНІ ПЕРЙОДАТИ І НАТРІЮ ПЕРКАРБОНАТ У ПЕРЕДОВИХ ПРОЦЕСАХ ОКИСНЕННЯ ОРГАНІЧНИХ ЗАБРУДНЮВАЧІВ ВОДНИХ СЕРЕДОВИЩ. ОГЛЯД

Анотація. *Розглянуто методи активації перйодатів і натрію перкарбонату для планування стратегічних підходів до підвищення ефективності й інтенсивності окиснювальної деградації органічних забруднювачів водних середовищ. Запропоновано класифікацію методів активації перйодатів на методи активації зовнішніми енергетичними впливами, методи каталітичної активації й інші методи активації (водню пероксидом, гідроксиламіном, у лужних умовах). Методи активації натрію перкарбонату поділено на методи гомогенної та гетерогенної активації.*

Ключові слова: *активація; перйодат; натрію перкарбонат; передові процеси окиснення; ультразвук; каталізатор.*